

Fabrication of Aluminum/Alumina Patterns using Localized Anodization of Aluminum

Jongho Park¹, Jacques Fattaccioli¹, Hiroyuki Fujita¹ and Beomjoon Kim^{1,#}

¹ CIRMM, Institute of Industrial Science, The University of Tokyo, 4-6-1, Komaba, Meguro-ku, Tokyo, Japan, 153-0041
Corresponding Author / E-mail: bjoonkim@iis.u-tokyo.ac.jp, TEL: +81-3-5452-6226, FAX: +81-3-5452-6225

KEYWORDS: Localized, Anodization, Alumina, Aluminum, Microelectrodes

In this paper, we investigated the localized anodization of aluminum evaporated on silicon substrate using micro scale patterns. Positive (S1818) and negative (SU-8 2035, KMPR 1010, KMPR 1035) photoresist patterns as well as SiO₂ micro patterns were fabricated on aluminum substrates respectively. Then, anodization of each substrate was performed in oxalic acid electrolyte. We observed the formation of aluminum/alumina patterns on a flat substrate by SEM images of its cross-section. This work provides an easy and simple technique for the fabrication of aluminum/alumina micro patterns by localized anodization.

Manuscript received: July 23, 2011 / Accepted: November 23, 2011

1. Introduction

Anodic aluminum oxide formed by the anodization, which is also known as anodic oxidation, has attracted continuous attention for many technical applications in nanotechnology field.^{1,2} Anodic alumina (aluminum oxide), formed by anodization in acidic electrolyte, is usually composed of hexagonally arranged cells with cylindrical pores in their center.³ Anodized porous alumina has been studied for many years and several mechanisms have been proposed to explain its unique structure and formation.⁴⁻⁶ The aluminum anodization process has been used for the fabrication of well-organized nano-sized pore structures⁷ as well as highly ordered nano templates.⁸⁻¹⁰

To pattern such aluminum oxide structures, local anodization of aluminum can be used. Localized anodization of pre-patterned aluminum layers have been used for the fabrication of planar interconnections¹¹ and arrays of alternating regions of aluminum and porous aluminum oxide.¹² Those reported localized anodization methods are based on the introduction of the mask that can prevent the formation of anodic alumina under protected areas. Typical materials used as a mask includes thin barrier anodic alumina layer fabricated using photoresist patterns,^{12,13} SiO₂ layer,^{6,14,15} niobium,¹⁶ and tantalum.¹⁷

Photoresists (e.g. S1805, S1818) and photosensitive epoxy type photoresists (e.g. SU-8TM, KMPR) are well known, and widely used for conventional micro electro mechanical systems (MEMS) fabrication. In particular, SU-8TM and KMPR have been used for

the fabrication of high aspect ratio micro structures due to its chemical resistance and compatibility with electroplating.¹⁸

In this work, we describe the localized anodization process for the formation of aluminum/alumina patterns by localized anodization. This procedure utilizes various photoresists such as S1818, SU-8 2035, KMPR 1010, and KMPR 1035 to fabricate anodization mask patterns. Then, localized anodization was performed with the patterned mask. Process parameters such as electrolytes used, anodizing temperature, and time which can influence anodization results were investigated. Finally, patterned aluminum/alumina structures were fabricated and the cross section of each substrate was observed by SEM. The aluminum/alumina patterns formed by this localized anodization process can be utilized for the fabrication of microelectrodes over large areas and the local formation of nano porous structures in micro patterns.

2. Fabrication Methods

3-inch silicon wafers were firstly cleaned using a sulfuric acid-hydrogen peroxide mixture (H₂SO₄:H₂O₂=1:1, v/v). Then, the wafers were thermally oxidized for 40 min at 1100°C in a wet oxidation condition with the oxygen flow rate of 1.5 L/min to grow a 300 nm thick SiO₂ layer. This silicon dioxide layer was used as the adhesion layer between the aluminum layer and the silicon substrate, which prevents the detachment of the alumina layer.

Titanium and platinum were deposited on SiO₂ using sputtering to a thickness of 50 nm each. They were used as interfacial layers between the SiO₂ and aluminum layer. Then, 1.2 μm thick aluminum was deposited at the deposition rate of 1 nm/s using thermal evaporation.

Four different photoresist layers, a 2 μm thick S1818 (MicroChem, Corp.) layer, a 40 μm thick SU-8 2035 (MicroChem, Corp.) layer, 10 μm thick KMPR 1010 (MicroChem, Corp.) layer, and 35 μm thick KMPR 1035 (MicroChem, Corp.) layer were patterned respectively on the aluminum layer by conventional photolithography. For comparison, a 200 nm thick SiO₂ layer was also deposited by a sputter deposition and patterned by photolithography and reactive ion etching.

Anodization was performed in a custom built electrochemical cell unit. A two-step anodization process that typically results in well-organized pore structures were not necessary here, since the purpose of this study is to develop a patterned aluminum/alumina formation process. Thus, the anodization process was carried out only one time in this work. Patterned samples were placed in a 0.3 M oxalic acid electrolyte at 1°C with stirring at 600 rpm. The samples were used as the anode and a platinum wire mesh (Nilaco, Co.) was employed as the cathode in the anodization process. The voltage between the cathode and the anode was applied using DC system power supply (N5751A, Agilent Technologies, Inc.). Digit Multimeter (Model 2000 6-1/2-Digit DMM, Keithley Instruments, Inc.) with a GPIB interface and Matlab (The MathWorks, Inc.) was used to measure the voltage and the current during anodization. Anodization voltage was gradually increased at the rate of 0.2 V/min and finally maintained to 40 V until the end of anodization. The total geometric area of each sample subjected to anodization was set to 4 cm². Anodization time was adjusted from 5 to 30 min with the interval of 5 min for each sample to confirm the morphological change of aluminum. As a final result, the anodic alumina was formed only in the areas where aluminum was exposed. After anodization was completed, samples were washed with deionized (DI) water and dried using nitrogen gas. The surface morphology and cross sections of aluminum/alumina patterns were investigated using scanning electron microscope (JSM-7400F, JEOL, Ltd.).

3. Results and Discussion

3.1 Interfacial layer compositions

Firstly, we checked how different interfacial layers between Si substrate and aluminum layers influence anodization results. The result is summarized in Table 1.

In Case 1 (Si/Al, Si/Ti/Al) where Ti layer was used as an interfacial layer, anodization process finished normally without any current surges, bubbles, or aluminum layer damages. Ti layer, which is oxidized under the operating conditions for anodization, also can be used to induce an electrochemical process at the interface between the substrate and anodic alumina to remove the aluminum barrier layer for the templates of nanowire

Table 1 The layer compositions and anodization results

Layers		Anodization results
1	Si/Al	Anodization process finished normally without any current surges, bubbles, or aluminum layer damages
	Si/Ti/Al	
2	Si/SiO ₂ /Al	Current surge and bubbles were observed Aluminum layer was severely damaged
	Si/SiO ₂ /Ti/Al	
3	Si/Pt/Al	Current surge and bubbles were observed Aluminum layer was severely damaged
	Si/SiO ₂ /Ti/Pt/Al	

Table 2 Parameters for anodization

Aluminum thickness (μm)	1.2
Voltage (V)	40
Current density (mA/cm^2)	1.25
Pore diameter (nm)	33~79
Submerged area (cm^2)	4
Film growth rate (nm/min)	32.55

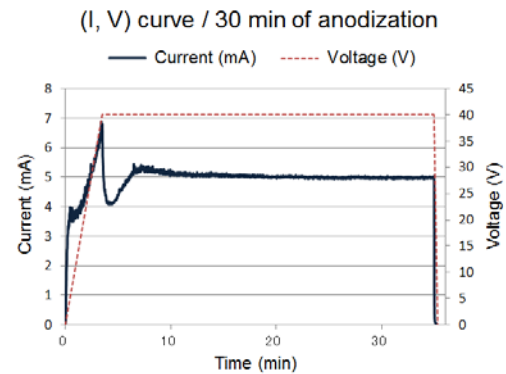


Fig. 1 Representative (I-V) curve during anodization

fabrications.¹⁹

Case 2 (Si/SiO₂/Al, Si/SiO₂/Ti/Al) is to show that the SiO₂ layer was deposited as the interfacial layer. SiO₂ layer is known to work as the adhesion layer between the aluminum layer and the substrate.²⁰

In case 3, we employed Pt layer and Ti/Pt layer as interfacial layers and found that Pt layer causes a sudden current increase, bubble formation and damage of the aluminum layer, which result from its anodic behavior. Those damages lead to a selective barrier layer etching without getting the porous layer damaged. As such characteristic of Pt layer is not necessary in this work, we excluded a Pt layer from the interfacial layers.

Based on the results above, we finally chose Si/SiO₂/Al layer composition to prepare aluminum substrates in following anodization experiments for this work.

3.2 Localized anodization with S1818 mask

The parameters for anodization are summarized in Table 2.

We recorded the current and voltage data during anodization using MATLAB and observed that I-V curve graph (Fig. 1) was consistent with typical anodization I-V curves.

After S1818 micro patterns on aluminum layer are fabricated, patterned samples were cut to make the submerged areas in the electrolyte of each sample constant. In addition, we coated edges of each sample with nail polisher to avoid the contact between exposed layers on its side and the electrolyte.

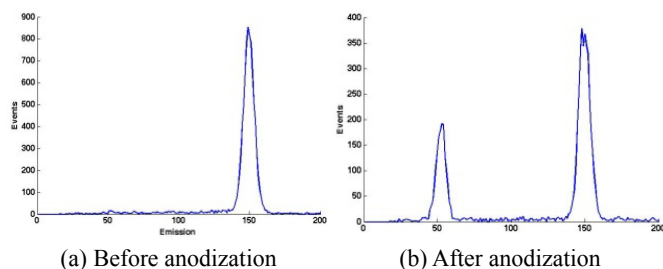


Fig. 2 EDX spectra before and after anodization

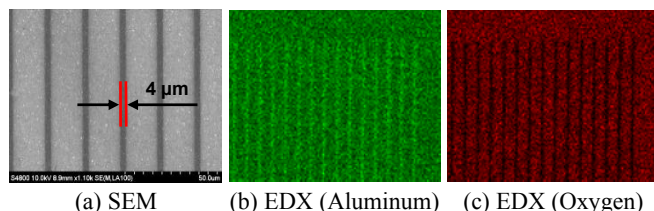


Fig. 3 SEM and EDX images of anodized samples (for (a), black lines: aluminum, gray thick lines: anodic alumina)

We confirmed anodization process, aluminum is oxidized and changed into anodic alumina, with the Field Emission SEM including Energy Dispersive X-ray (EDX) Spectrometer (S-4800 UHR FE-SEM, Hitachi, Inc.). The EDX spectrometer gives the chemical composition of the sample with 1 μm lateral resolution. Fig. 2 shows EDX spectra of aluminum (Fig. 2(a)) and anodic alumina where the oxygen peak appears (Fig. 2(b)).

Fig. 3 shows the SEM and the X-ray analysis (EDX) image of the samples after anodization. The contrast between aluminum and anodized alumina is confirmed with 4 microns of a line pattern. We found that anodized alumina parts have oxygen atoms (Fig. 3(c)). On the contrary, masked parts, which are not anodized, have only aluminum atoms (Fig. 3(b)). As a result, we confirmed that localized anodization with a pre-patterned mask is feasible for the fabrication of aluminum/alumina micro patterns.

Then, we observed the surface of anodic alumina and its cross section with respect to the anodization time using SEM (Fig. 4). The growth rate of anodic alumina with our experimental setup was calculated at 32.55 nm/min by SEM observation of anodized samples. Anodic oxidation of aluminum layers started in the uncovered region at first. As anodization progresses, pores of anodic alumina near the S1818 covered regions tend to grow in tilted direction. As electrical potential increases with the formation of barrier layer, electric field deflection occurs beneath the S1818 mask regions due to its insulating characteristic.¹⁴

Next, we performed the anodization until the aluminum layer was anodized fully (Fig. 5). We found that S1818 pattern was peeled off partially during anodization and confirmed it from SEM images (Fig. 5(a), red dotted line: traces of S1818 patterns). From Fig. 5(b), we observed that anodization process started newly from where S1818 patterns were peeled off during anodization. Based on the film growth rate of previous experiments and the thickness where S1818 was patterned, the time when anodization newly started was calculated at 21 min after S1818 started to be peeled off.

Regarding this calculation, we also confirmed from I-V curves

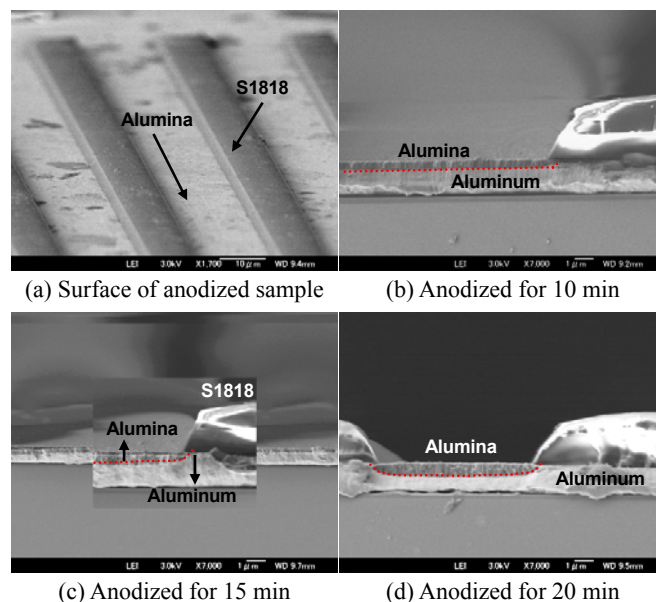


Fig. 4 Anodized samples with S1818 patterns

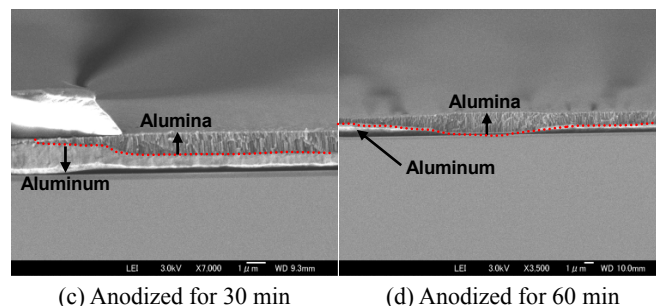
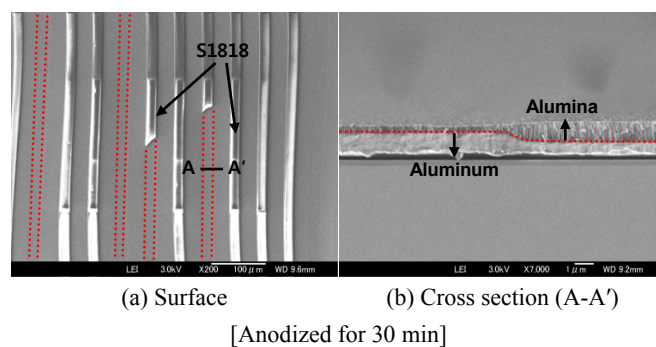


Fig. 5 Anodized samples over 30 min with S1818

that the current started to increase after 21 min, the time when S1818 started to be peeled off, and kept increasing until the anodization ends. In our experiment, 1.2 μm thick aluminum layer was fully anodized in 89 min after anodization firstly started.

In addition, we found that small gap between aluminum layer and SiO_2 layer in the parts where anodization was not fully finished. However, once the anodization completed and aluminum converted to anodic alumina fully, there were no gap between anodic alumina and SiO_2 layer. We suppose that the gap was caused by the mechanical sample cutting or volume expansions of anodic alumina occurred during anodization process.

With our experimental results, we concluded that S1818 mask patterns are effective for at least 20 min under the harsh anodization environment (1°C, 0.3 M of oxalic acid, 600 rpm).

3.3 Localized anodization with SU-8 2035 mask

For the next step, we performed anodization with SU-8 2035 patterned mask. The parameters used for anodization were same as the anodization with S1818 mask.

We found that most of SU-8 patterns started to be peeled off with beginning anodization process. Anodization was stopped after 10 min to observe the surface of samples by SEM. SEM images show that SU-8 patterns were removed or damaged severely, which results in no localized anodization occurred (Fig. 6(a), (b)). We suppose that the adhesion between SU-8 and aluminum layer was not strong enough to endure harsh anodization environment. Thus, we tried Omnicoat™ (MicroChem, Corp.) to enhance the adhesion between SU-8 and aluminum layer. But, results show that there left only traces of SU-8 patterns and finally localized anodization was not done (Fig. 6(c)).

We concluded that the thickness of SU-8 2035 patterns, which is relatively thicker (40 μm) than S1818 (2 μm), contributed to the loss of patterns under harsh anodization environment. Therefore, we tried KMPR negative photoresist for better adhesion and durability for the next mask material.

3.4 Localized anodization with KMPR 1010, 1035 mask

As we have adhesion problems with SU-8 2035 during anodization, we chose KMPR 1010 and 1035 photoresists as the alternative. KMPR series photoresists show better adhesion on aluminum substrates than SU-8.²⁰ In addition, the thickness of evaporated aluminum was adjusted to 400 nm to reduce the time for anodization which results in the decrease of damages to samples in harsh anodizing conditions.

We fabricated micro patterns with 20 μm of line width and space. We performed localized anodization with KMPR patterns for 18 min and observed the results (Fig. 7). The growth rate of anodic alumina with KMPR patterns was 31.42 nm/min. All KMPR photoresists were intact during anodization. It is well known that anodic alumina expands during anodization of aluminum.¹²⁻¹⁴ We confirmed that the results of localized anodization with S1818, SU-8, and KMPR photoresist patterns show the volumetric expansion during anodization (Fig. 7(b), (c)). Tilted pore growths near the boundary of each photoresist pattern, which we observed from the results of anodization with S1818, were observed here. Furthermore, we also observed a small void, which is very similar to the result of S1818 pattern masks, between KMPR patterns and aluminum layer (Fig. 7(d), red box). We suppose that both edges at the bottom of patterns were raised up as pores grow in a tilted direction with volumetric expansion. But, KMPR patterns did not peel off and show any adhesion problems until the end of anodization.

3.5 Localized anodization with SiO₂ mask

The researches related with the anodization with SiO₂ mask were published by several research groups.^{6,14,15} We also performed the localized anodization with SiO₂ patterned mask to compare it with the results with other photoresist masks (Fig. 8).

We expect the anodization results with S1818, KMPR and SiO₂ mask will very similar because all materials are electrical insulators

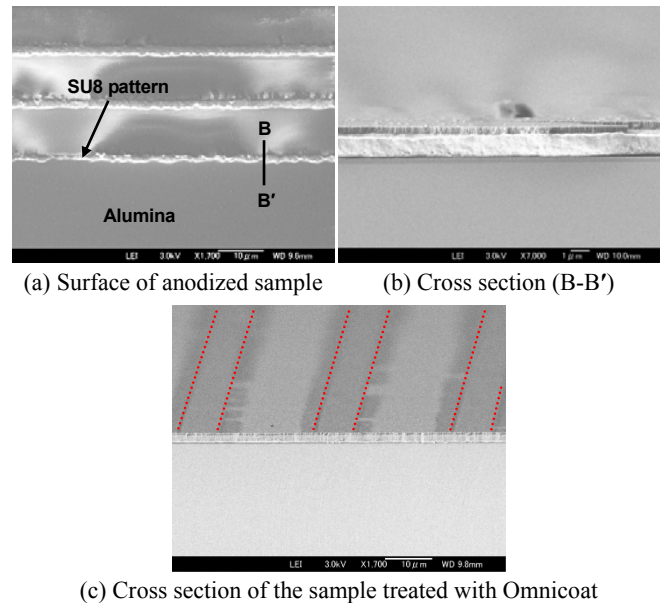


Fig. 6 Anodized sample with SU-8 pattern mask

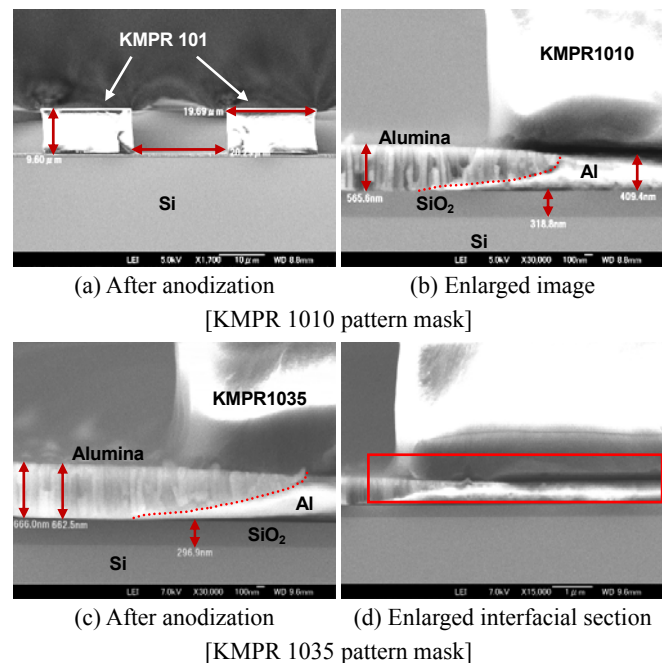


Fig. 7 Anodized sample with KMPR pattern mask

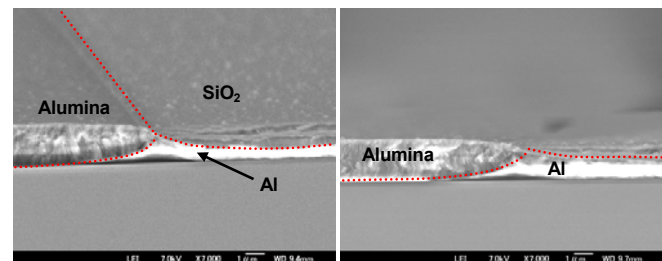


Fig. 8 Anodized sample with SiO₂ pattern mask

which can cause the deflection of electrical field in common. As we expected, results with SiO₂ mask were found to be very similar with those of S1818 or KMPR mask. Tilted pore structures of anodic alumina around the boundary and volumetric expansion were also

observed here. In addition, SiO₂ mask was intact throughout whole anodization process. However, localized anodization with SiO₂ mask has two additional processes, which include the deposition SiO₂ by sputtering and the removal of it using wet or dry etching.

4. Conclusions

In this work, we performed localized anodization by mask patterns on aluminum layer. S1818, SU-8 2035, KMPR 1010, and KMPR 2035 photoresists were used for mask material and patterned by conventional photolithography. For comparisons of results, we also performed localized anodization with SiO₂ mask. We observed that the localized anodization with S1818, KMPR, and SiO₂ mask patterns were similar with each other. But, localized anodization with SU-8 mask was not done due to the loss of SU8 patterns under harsh anodization environment. KMPR and SiO₂ mask were intact during anodization, whereas S1818 mask was intact for at least 20 min from the beginning of anodization. We observed tilted pore growths near the boundary of mask patterns and volumetric expansion during anodization. Yet, we found it is difficult to fabricate vertically selective anodization of aluminum with high aspect ratio due to the deflective growth of alumina. As further study, we will confirm that aluminum/alumina patterns by localized anodization can be used in the fabrication of microelectrodes over large areas and the local formation of nano porous structures in micro patterns by controlling fabrication conditions. In addition, we are planning to perform the localized anodization on the nonplanar surface by using flexible microstencil²¹ or flexible photo mask by optical-soft lithography.²²

ACKNOWLEDGEMENT

We greatly appreciate the technical support and the cooperation from Namiki Precision Jewel Co., Ltd. We also would like to thank Kazuya Nakamura (Namiki Precision Jewel Co., Ltd.) for valuable comments and fruitful discussions.

REFERENCES

1. Diggle, J. W., Downie, T. C. and Goulding, C. W., "Anodic Oxide Films on Aluminum," *Chem. Rev.*, Vol. 69, No. 3, pp. 365-405, 1969.
2. Li, F., Zhang, L. and Metzger, R. M., "On the Growth of Highly Ordered Pores in Anodized Aluminum Oxide," *Chem. Mater.*, Vol. 10, pp. 2470-2480, 1988.
3. Masuda, H. and Fukuda, K., "Ordered Metal Nanohole Arrays Made by a Two-step Replication of Honeycomb Structures of Anodic Alumina," *Science*, Vol. 268, No. 5216, pp. 1466-1468, 1995.
4. Keller, F., Hunter, M. S. and Robinson, D. L., "Structural Features of Oxide Coatings on Aluminum," *J. Electrochem. Soc.*, Vol. 100, No. 9, pp. 411-419, 1953.
5. Thompson, G. E. and Wood, G. C., "Anodic Films on Aluminum in Treatise on Materials Science and Technology," Academic Press, pp. 205-329, 1983.
6. Huang, Q., Lye, W.-K. and Reed, M. L., "Mechanism of Isolated Pore Formation in Anodic Alumina," *Nanotechnology*, Vol. 18, No. 40, Paper No. 405302, 2007.
7. Lee, W., Ji, R., Gösele, U. and Nielsch, K., "Fast Fabrication of Long-range Ordered Porous Alumina Membranes by Hard Anodization," *Nat. Mater.*, Vol. 5, pp. 741-747, 2006.
8. Myung, N. V., Lim, J., Fleurial, J.-P., Yun, M., West, W. and Choi, D., "Alumina Nanotemplate Fabrication on Silicon Substrate," *Nanotechnology*, Vol. 15, No. 7, pp. 833-838, 2004.
9. Choi, J., Sauer, G., Nielsch, K., Wehrspohn, R. B. and Gösele, U., "Hexagonally Arranged Monodisperse Silver Nanowires with Adjustable Diameter and High Aspect Ratio," *Chem. Mater.*, Vol. 15, No. 3, pp. 776-779, 2003.
10. Shingubara, S., "Fabrication of Nanomaterials Using Porous Alumina Templates," *J. Nanopart. Res.*, Vol. 5, No. 1-2, pp. 17-30, 2003.
11. Schwartz, G. C. and Platter, V., "An Anodic Process for Forming Planar Interconnection Metallization for Multilevel LSI," *J. Electrochem. Soc.*, Vol. 122, No. 11, pp. 1508-1516, 1975.
12. Barela, M. J., Brevnov, D. A., Bauer, T. M., López, G. P. and Atanassov, P. B., "Fabrication of Patterned Arrays with Alternating Regions of Aluminum and Porous Aluminum Oxide," *Electrochem. Solid-State Lett.*, Vol. 8, No. 1, pp. C4-C5, 2005.
13. Brevnov, D. A., Womack, R. L., Atanassov, P., López, G. P., Bauer, T. M., Chaudhury, Z. A., Schwappach, C. D. and Mosley, L. E., "Width of Anodization Mask Required to Preserve a Metallic Phase during Porous-Type Anodization of Aluminum-Copper Films," *J. Electrochem. Soc.*, Vol. 153, No. 3, pp. B108-B112, 2006.
14. Zhao, X., Jiang, P., Xie, S., Liu, L., Zhou, W., Gao, Y., Song, L., Wang, J., Liu, D., Dou, X., Luo, S., Zhang, Z., Xiang, Y. and Wang, G., "Anodizing Behavior of Aluminum Foil Patterned with SiO₂," *J. Electrochem. Soc.*, Vol. 152, No. 10, pp. B411-B414, 2005.
15. Sharma, G., Chong, S. C., Ebin, L., Hui, C., Gan, C. L. and Kripesh, V., "Fabrication of Patterned and Non-patterned Metallic Nanowire Arrays on Silicon Substrate," *Thin Solid Films*, Vol. 515, No. 7-8, pp. 3315-3322, 2007.
16. Lazarouk, S., Baranov, I., Maiello, G., Proverbio, E., De Cesare, G. and Ferrari, A., "Anisotropy of Porous Anodization of Aluminum for VLSI Technology," *J. Electrochem. Soc.*, Vol. 141, No. 9, pp. 2556-2559, 1994.

17. Zhao, X., Jiang, P., Xie, S., Feng, J., Gao, Y., Wang, J., Liu, D., Song, L., Liu, L., Dou, X., Luo, S., Zhang, Z., Xiang, Y., Zhou, W. and Wang, G., "Patterned Anodic Aluminium Oxide Fabricated with a Ta mask," *Nanotechnology*, Vol. 17, No. 1, pp. 35-39, 2006.
18. Lorenz, H., Despont, M., Fahrni, N., LaBianca, N., Renaud, P. and Vettiger, P., "SU-8: A Low-cost Negative Resist for MEMS," *J. Micromech. Microeng.*, Vol. 7, No. 3, pp. 121-124, 1997.
19. Rabin, O., Herz, P. R., Lin, Y. M., Akinwande, A. I., Cronin, S. B. and Dresselhaus, M. S., "Formation of Thick Porous Anodic Alumina Films and Nanowire Arrays on Silicon Wafers and Glass," *Adv. Funct. Mater.*, Vol. 13, No. 8, pp. 631-638, 2003.
20. Blanco Carballo, V. M., Melai, J., Salm, C. and Schmitz, J., "Moisture resistance of SU-8 and KMPR as structural material," *Microelectron. Eng.*, Vol. 86, No. 4-6, pp. 765-768, 2009.
21. Choi, J. H. and Kim, G. M., "Micro-Patterning on Non-Planar Surface using Flexible Microstencil," *Int. J. Precis. Eng. Manuf.*, Vol. 12, No. 1, pp. 165-168, 2011.
22. Park, J., Fujita, H. and Kim, B., "Fabrication of Metallic Microstructure on Curved Substrate by Optical Soft Lithography and Copper Electroplating," *Sensors and Actuators A: Physical*, Vol. 168, No. 1, pp. 105-111, 2011.